J Mol Model (2016) 22: 70
DOI 10.1007/s00894-016-2954-8

ORIGINAL PAPER

N–H bond cleavage of ammonia on graphene-like B_{36} borophene: DFT studies

Zahra Rostami[1] · **Hamed Soleymanabadi**[2]

Received: 9 January 2016 / Accepted: 29 February 2016 / Published online: 11 March 2016

Abstract Ammonia N–H bond cleavage at metal-free substrates has attracted great attention because of its industrial importance. Here, we investigate the dissociative adsorption of ammonia onto the surface of a B_{36} borophene sheet by means of density functional theory calculations. We show that the N–H bond may be broken at the edges of B_{36} even at room temperature, regarding the small energy barrier of 14.1–19.3 kcal mol^{-1} at different levels of theory, and more negative Gibbs free energy change. Unlike basis set size, the kind of exchange correlation functional significantly affects the electronic properties of the studied systems. Also, by increasing the percentage of Hartree Fock (HF) exchange of density functionals, the activation and adsorption energies are lowered. A linear relationship between the highest occupied molecular orbital or lowest unoccupied molecular orbital of B_{36} borophene and the %HF exchange of functionals is predicted. Our work reveals that pure whole boron nanosheets may be promising metal-free materials in N–H bond cleavage, which would raise the potential application of these sheets.

Keywords Graphene-like · Nanostructure · Self-interaction error · Boron compound

Electronic supplementary material The online version of this article (doi:10.1007/s00894-016-2954-8) contains supplementary material, which is available to authorized users.

✉ Zahra Rostami
zahrarostami.pnu@gmail.com

[1] Department of Chemistry, Payame Noor University (PNU), PO Box, 19395-3697 Tehran, Iran

[2] Young Researchers and Elite Club, Shahre-Rey Branch, Islamic Azad University, Tehran, Iran

Introduction

Ammonia N–H bond cleavage is a first rung, not only in the transformation of abundant ammonia into a valuable amino compound, but also in the start of numerous catalytic reactions [1, 2]. Conventional N–H bond cleavage methods depend mainly on the different transition metal centers [2]. But toxicity problems, high cost and simple Lewis acid–base adducts formation with transition metals impose great limitations on the possible applications as an NH_3 splitter [3]. Therefore, researchers have attempted to find metal-free ammonia splitters. Recently, nanostructured materials have invoked extensive interest as substrates due to their unique properties, such as high surface to volume ratio, and exclusive electronic properties [4–10]. Using density functional theory (DFT) calculations, Ding et al. [3] demonstrated that pristine SiC nanotubes can break the ammonia N–H bond by molecular chemisorption, releasing energy of ~1.370 eV. The latter authors used the Perdew Burke Ernzerhof (PBE) exchange correlation density functional with double numerical basis sets plus polarization functional (DNP) [3]. Using the B3LYP/6-31G (d) method, it has been revealed that open-ended BN nanotubes can cleave the N–H bond of ammonia via a two-step mechanism [11].

Numerous studies to date have focused on graphene-like boron nanosheets because they are of similar interest as graphene [12–14]. It has been shown that the B atoms cannot form a honeycomb hexagonal nanosheet because of electron deficiency [15]. In 2004, Piazza et al. [15] reported the synthesis of a quasiplanar whole boron sheet with a central hexagonal hole. They found that this neutral B_{36} sheet is a highly stable sheet with C_{6v} symmetry, extension of which would afford larger planar boron nanosheets with hexagonal vacancies. Following this report, B_{36} borophene has attracted considerable attention from the scientific community [16–18]. For example, based on the DFT calculations, Liu et al. [17] have

shown that metallized B_{36} borophene can serve as reversible hydrogen storage. At the B3LYP level, the adsorption of CO, N_2, H_2O, O_2, H_2 and NO molecules on B_{36} borophene has been explored [18]. In this work, by performing DFT calculations at different levels and with different basis sets, we examine the potential application of B_{36} borophene as a metal free NH_3 splitter

Computational details

Energy predictions, transition state calculations and geometry optimizations on a B_{36} and different NH_2–B_{36}–H complexes were performed using B97D level [19] of theory with 6-31G (d) basis set as implemented in the GAMESS suite of program [20]. Vibrational frequency analysis was performed at the same level of theory to confirm that all structures were in true local minimum, and also to obtain thermodynamic data. Molecular electrostatic potential (MEP) [21, 22], nuclear magnetic resonance (NMR), and natural bond orbital (NBO) analyses were done at B97D level with the 6-311++G (d, p) basis set. Also, the effect of different exchange correlation density functionals and basis sets were explored.

We defined adsorption energy as:

$$E_{ad} = E\,(NH_2\text{-}B_{36}\text{-}H) - E\,(B_{36}) - E\,(NH_3) \quad (1)$$

where E (NH_2–B_{36}–H) corresponds to the electronic energy of the NH_2–B_{36}–H complex, E (B_{36}) is the energy of the isolated fullerene, and E (NH_3) is the energy of a single NH_3. The HOMO–LUMO energy gap is defined as

$$E_g = E_{LUMO}\text{-}E_{HOMO} \quad (2)$$

where E_{LUMO} and E_{HOMO} are the energy of the lowest unoccupied molecular orbital (LUMO and highest occupied molecular orbital (HOMO), respectively. The change in the HOMO–LUMO gap, as an index of the electronic sensitivity of the B_{36} toward the dissociative adsorption of ammonia, is obtained by:

$$\Delta E_g = \left[\left(E_{g2}\text{-}\,E_{g1}\right)\Big/E_{g1}\right] * 100 \quad (3)$$

where E_{g1} and E_{g2} are, respectively, the value of E_g in the initial and the final state.

Results and discussion

In Fig. 1, the optimized geometry of the B_{36} sheet indicates that it is not completely planar and has a curvature that was first synthesized and reported by Piazza and co-workers [15]. Five kinds of boron atoms can be detected on a trapezoid shape (Fig. 1) based on B-11 NMR analysis. The calculated NMR chemical shifts for B1, B2, B3, B4, and B5 atoms (Fig. 1) are about 121.5, 120.9, 57.8, 91.4, and 86.1 ppm, respectively. The structure includes a central hexagon with C_{6v} symmetry. This symmetry degenerates the energy levels so that the HOMO and LUMO are two-fold degenerated levels (Fig. 2), which lie at −5.12 and −4.01 eV, respectively. Thus, the calculated HOMO–LUMO gap is about 1.11 eV at B97D level of theory. The MEP maps (Fig. 1) show that inner side of the sheet is much more negatively charged in comparison to the outer side, hence the outer site will be more appropriate for a nucleophilic NH_3 molecule attack. Different bonds in the range of 1.59 to 1.75 Å exist, with B3–B4 and B4–B3 (Fig. 1) being the largest and shortest bonds, respectively. Using PBE0/6-31G(d) level of theory, Piazza et al. [15] showed that neutral B_{36} has perfect hexagonal symmetry ($©_{6v}$), and is overwhelmingly stable relative to the closest-lying isomers. They indicated that the shortest bond length occurs between the six apex B atoms and their neighbors (1.58 Å), while the remaining six peripheral B–B bonds are slightly longer (1.67 Å). Based on our results, the vibrational frequency modes are in the range of 108–1282 cm^{-1}, indicating that B_{36} is in a true local minimum on the potential energy surface.

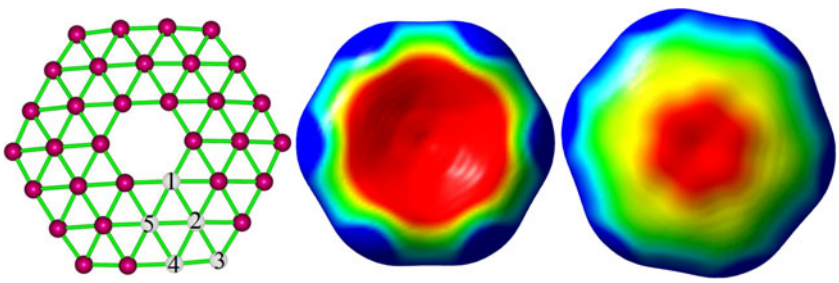

Fig. 1 Optimized structure of B_{36} borophene and its inner and outer molecular electrostatic potential maps. The surface is defined by the 0.0004 electrons b^{-3} contour of the electronic density. Color ranges (in a.u.): *blue* more positive than 0.010, *green* between 0.010 and 0, *yellow* between 0 and −0.010, *red* more negative than −0.010

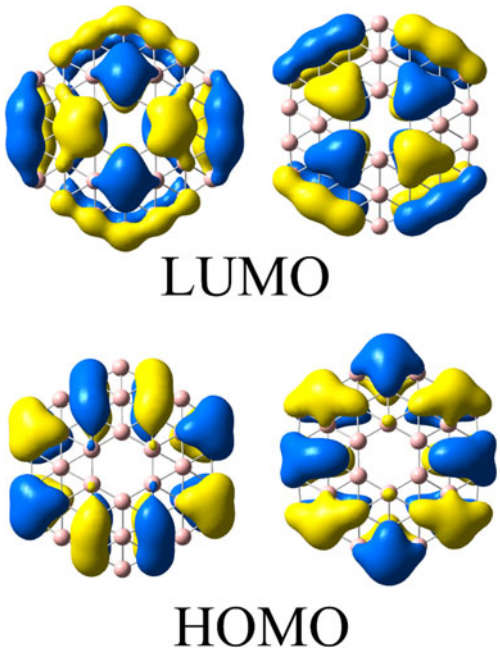

Fig. 2 The two-fold degenerated highest occupied molecular orbital (HOMO) and lowest unoccupied molecular orbital (LUMO) profiles of B_{36} borophene

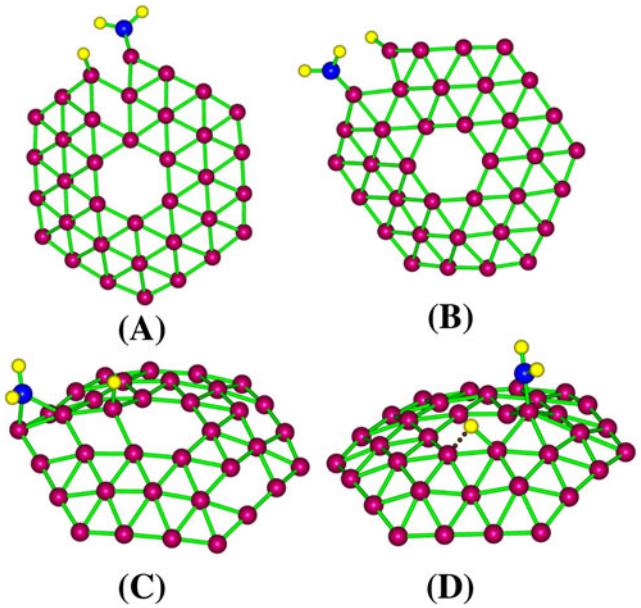

Fig. 3 Optimized structures of different H–B_{36}–NH_2 complexes

To explore N–H bond cleavage on the surface of borophene, we investigated the feasibility of different cleavage from the standpoint of thermodynamics and kinetics. Towards this aim, we first assumed that an NH_3 molecule dissociates into two fragments, –H and –NH_2, attacking different B–B bonds. Figure 3 illustrates the four most stable predicted complexes with positive frequencies. Among these complexes, the most stable complex (**A**) is that in which the ammonia molecule attacks the B3–B4 bond, and hydrogenates the B4 atom, retaining the –NH_2 group on the B3 atom. The adsorption energy for this process is about −42.7 kcal mol^{-1}, demonstrating a favorable reaction. In the second most stable complex (**B**), in contrast to complex **A**, the B3 atom is hydrogenated and the NH_2 group is attached to the B4 atom with adsorption energy of −24.5 kcal mol^{-1}. The higher stability of complex **A** compared to **B** shows that the nucleophilic –NH_2 group tends to attach to the B3 atom because it is three-fold coordinated while the B4 atom is four-fold coordinated. In the next most stable structure (**C**), the B1 atom is hydrogenated and the –NH_2 group shifts on the B2–B3 bond and forms a bridge with adsorption energy of about −17.38 kcal mol^{-1}. Upon the adsorption process, a strong structure deformation occurs and the B1–B2–B3 fragment is projected out. For complex (**D**) the adsorption energy is positive (+13.91 kcal mol^{-1}), indicating that the complex formation is energetically unfavorable. In this complex, the ammonia dissociates on the B atoms of central hexagon so that –NH_2 attaches to a B atom and –H shifts to the adjacent B–B bond. Generally, complexes (**C** and **D**) in which the central hexagon participates in the reaction are less favorable.

Here, we will focus on the energetically most stable complex (**A**). In this complex, two new bonds including B–H and B–NH_2, are formed with bond lengths of 1.21 and 1.40 Å, and Wiberg bonds index (WBI) [23] of 0.878 and 1.193, respectively, showing a covalent nature of the bonds formed. After the dissociative adsorption of ammonia, the B3–B4 bond was broken, so the bond length increased from 1.59 to 1.94 and the WBI from 1.137 to 0.534. The reaction yielding this complex was accompanied by a decrease in entropy, so the ΔS is about −0.034 kcal mol^{-1} K at room temperature and 1 Atm. Under these conditions, the change in Gibbs free energy (ΔG) is about −31.9 kcal mol^{-1}, indicating a thermodynamically favorable reaction. The vibrational frequency modes were calculated to be in the range of 46–3589 cm^{-1}. The B–H and B–N stretching modes appeared at 2579 and 1391 cm^{-1}, respectively, and the maximum vibrational mode belongs to the asymmetric stretch of H–N–H. The dissociative adsorption of ammonia significantly influences the electronic properties of the B36 borophene, especially the HOMO level. After the adsorption process, the LUMO does not change significantly but the HOMO jumps sharply to higher energies by about 0.35 eV. This narrows the HOMO–LUMO gap by about 37 %, reducing from 1.11 to 0.69 eV. The HOMO–LUMO gap is an important index in determining the electrical conductivity and kinetic stability of semiconductors [24–30].

It is well known that several properties depend on the density functional used, and there is no universal exchange-correlation density functional for all properties. Therefore, we inspected the effect of different density functionals on the energetic and electronic properties of B_{36} and complex **A**. For this purpose, the calculations were repeated with four Minnesota 06 functionals, including M06-L [31], M06 [32],

Table 1 The results of different density functionals with 6-31G (d) basis set for dissociation of NH_3 on B_{36} borophene. Activation (E_{act}) and adsorption (E_{ad}) are in kcal mol^{-1}, and the unit of electronic properties is eV. The E_g is HOMO–LUMO gap and ΔE_g is its change after the adsorption of NH_3

System	Functional	E_{ad}	E_{act}	E_{HOMO}	E_{LUMO}	E_g	ΔE_g(%)
B_{36}	M06-L (0)*	–	–	−5.41	−4.16	1.25	–
	M06 (27)	–	–	−5.75	−3.49	2.26	–
	M06-2X (54)	–	–	−6.56	−3.23	3.34	–
	M06-HF (100)	–	–	−7.70	−2.48	5.22	–
H-B_{36}-NH_2	M06-L(0)	−37.9	19.3	−5.05	−4.24	0.80	−35.6
	M06 (27)	−40.2	17.9	−5.39	−3.66	1.73	−23.5
	M06-2X (54)	−42.0	17.5	−6.16	−3.38	2.78	−16.7
	M06-HF (100)	−48.2	14.4	−7.25	−2.66	4.59	−12.2

*Numbers in parenthesis indicates the HF exchange percentage of density functional

M06-2X [32], and M06-HF [33], with 0, 27, 54, and 100 % Hartree Fock (HF) exchange, respectively. The results in Table 1 show that the HOMO, LUMO, and HOMO–LUMO gap depend strongly on the type of density functional used. In all systems, the HOMO and LUMO stabilized and destabilized, respectively, upon increasing the %HF exchange, thereby increasing the HOMO–LUMO gap. For instance, the HOMO, and LUMO of B_{36} against the %HF exchange of the functionals was plotted in Fig. 4, illustrating a linear relationship.

Also, by growing the %HF exchange, the ΔE_g value decreases (Table 1, Fig. 4). The ΔE_g is a key value in the calculation of sensitivity of an adsorbent toward a chemical and in estimating the semiconductor electrical transport [34–37]. Non-hybrid functionals (B97D and M06-L) predicts higher HOMO and lower LUMO, thereby giving a smaller HOMO–LUMO gap. The %HF exchange has quite a large effect on the adsorption energy, so that by increasing the %HF the adsorption energy becomes more negative. The different results are due to the charge delocalization error and many self-interaction errors of approximate density functionals [38]. Based on the adsorption energy dependency on the %HF, it seems that the charge delocalization and self-interaction errors are more stabilized than two separate NH_3, and B_{36} borophene more than the complex.

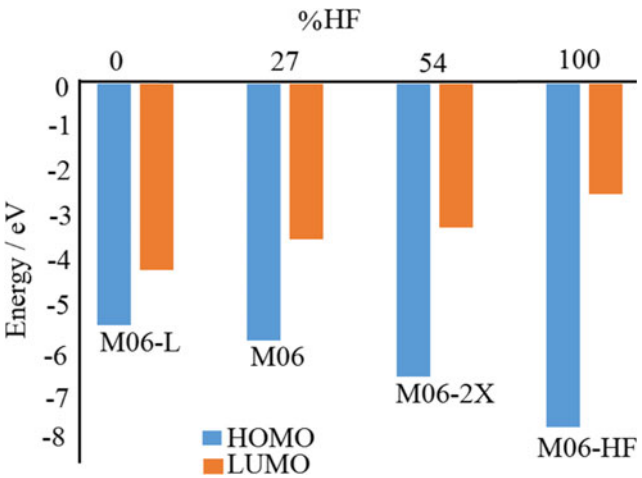

Fig. 4 The HOMO, and LUMO of B_{36} against the %HF exchange of the different functionals

We also probed the effect of different basis sets, including split-valence 6-31 + G(d), and 6-311++G(d,p), and correlation-consistent cc-pVDZ, and cc-pVTZ at the same B97D level of theory. The results in Table 2 show that enlarging the basis set by adding polarization or diffuse functions on hydrogen or heavy atoms slightly influences the adsorption energies, HOMO and LUMO levels, but it has no significant effect on the HOMO–LUMO gap and its change upon the adsorption process. The results of the correlation-consistent basis sets are in good agreement with those of split-valence. Generally, the results depend much more on the exchange correlation functional than on the basis set.

In the next step, we have explored the kinetic possibility of NH_3 dissociation on the B_{36} borophene. With this aim, we calculated the transition state structure using the synchronous transit-guided quasi-Newton (STQN) method [39]. Our calculations show that the NH_3 molecule moving toward the tube has to overcome an energy barrier of 17.4 kcal mol^{-1} before entirely breaking the N–H bond at the B_{36} edge. When the reaction reaches the TS structure (Fig. 5), the H–NH_2 bond is lengthened from 1.028 Å (in single NH_3) to 1.381 Å, and the corresponding WBI decreased to 0.352, representing a

Table 2 Results of different basis sets at B97D level for dissociation of NH_3 on the B_{36} borophene. Adsorption energy (E_{ad}) is in kcal mol^{-1}, and the unit of electronic properties are eV. The E_g is HOMO–LUMO gap and ΔE_g is its change after the adsorption of NH_3

System	Basis set	E_{ad}	E_{HOMO}	E_{LUMO}	E_g	ΔE_g(%)
B_{36}	6-31 + G(d)	–	−5.35	−4.25	1.10	–
	6-311++G(d,p)	–	−5.39	−4.30	1.09	–
	cc-pVDZ	–	−5.33	−4.23	1.09	–
	cc-pVTZ	–	−5.37	−4.29	1.09	–
H-B_{36}–NH_2	6-31 + G(d)	−39.7	−5.02	−4.34	0.68	−38
	6-311++G(d,p)	−37.2	−5.06	−4.38	0.68	−38
	cc-pVDZ	−43.5	−4.97	−4.29	0.68	−38
	cc-pVTZ	−38.5	−5.04	−4.36	0.68	−38

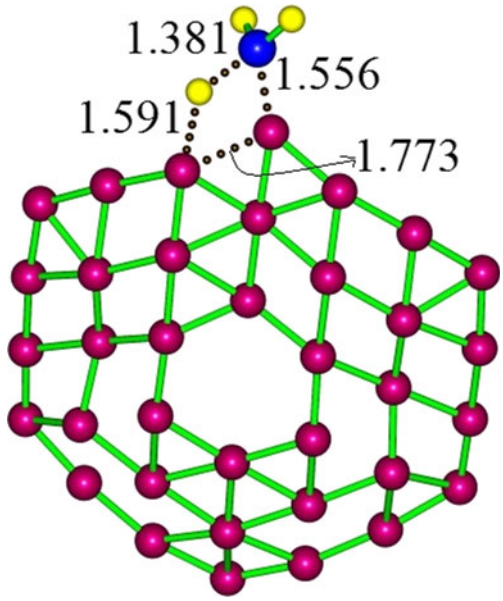

Fig. 5 The optimized structure of transition state of dissociation of ammonia molecule on the B_{36} borophene. Distances in Å

tendency for bond breaking. We predicted a strong negative vibrational mode at −1598 cm^{-1}, which corresponds to the coordination of detaching the –H atom from the NH_3 and attaching to the B atom of B_{36}. An animation of this mode is provided in the Supplementary material, which can be viewed with internet browser software.

The activation energy was calculated once again at the M06-L, M06, M06-2X, and M06-HF levels. Figure 6 shows a scheme of the reaction pathway for the dissociative adsorption of NH_3 on the B_{36} borophene at these levels. The zero energy level relates to the two reactants (NH_3 and B_{36}) being

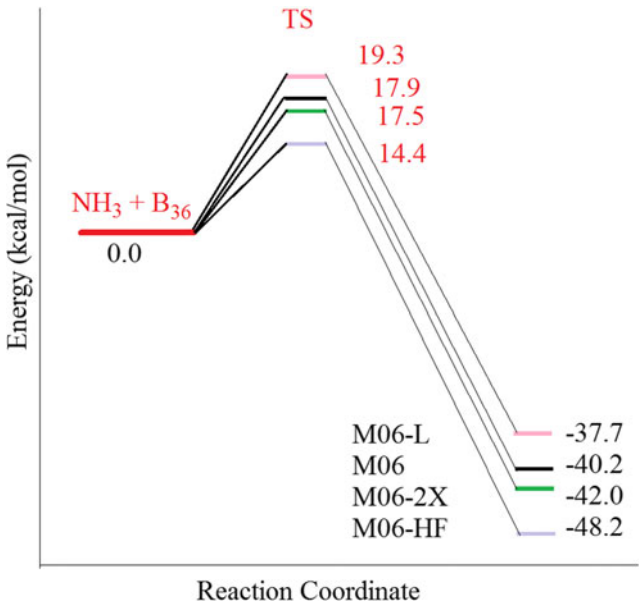

Fig. 6 A scheme of the reaction pathway for the dissociative adsorption of NH_3 on the B_{36} borophene at different levels

infinitely far from each other. The results indicate that, similar to the adsorption energy, the activation energy is lowered as the %HF increases. This is attributed to a reduction in the charge delocalization error in the separated species. It can be expected that the dissociative adsorption of NH_3 may be carried out even at room temperature, according to the small energy barrier and large adsorption energy.

Conclusions

Using DFT calculations at B97D, M06-L, M06, M06-2X, and M06-HF levels of theory, the dissociative adsorption of NH_3 on the surface of a B_{36} borophene was investigated. It was shown that this reaction may be carried out at room temperature, considering the small energy barrier of 14.1 kcal mol^{-1} and ΔG of −31.9 at B97D level of theory. The results reveal that the adsorption and activation energies are decreased and the HOMO–LUMO gap sharply increased by increasing the %HF exchange. Also, we predicted a linear relationship between the HOMO or LUMO of B_{36} borophene and the % HF exchange of functionals.

References

1. Nakajima Y, Kameo H, Suzuki H (2006) Cleavage of nitrogen–hydrogen bonds of ammonia induced by triruthenium polyhydrido clusters. Angew Chem Int Ed 45(6):950–952
2. Zhao J, Goldman AS, Hartwig JF (2005) Oxidative addition of ammonia to form a stable monomeric amido hydride complex. Science 307(5712):1080–1082
3. Zhao J-X, Xiao B, Ding Y-H (2009) Theoretical prediction of the N−H and O−H bonds cleavage catalyzed by the single-walled silicon carbide nanotube. J Phys Chem C 113(38):16736–16740
4. Moradi M, Peyghan AA, Bagheri Z, Kamfiroozi M (2012) Cation-π interaction of alkali metal ions with C_{24} fullerene: a DFT study. J Mol Model 18:3535–3540
5. Beheshtian J, Baei MT, Peyghan AA, Bagheri Z (2012) Electronic sensor for sulfide dioxide based on AlN nanotubes: a computational study. J Mol Model 18:4745–4750
6. Peyghan AA, Noei M, Tabar MB (2013) A large gap opening of graphene induced by the adsorption of Co on the Al-doped site. J Mol Model 19(8):3007–3014
7. Ahmadi A, Beheshtian J, Kamfiroozi M (2012) Benchmarking of ONIOM method for the study of NH3 dissociation at open ends of BNNTs. J Mol Model 18(5):1729–1734
8. Beheshtian J, Ahmadi Peyghan A, Bagheri Z (2013) Ab initio study of NH 3 and H 2 O adsorption on pristine and Na-doped MgO nanotubes. Struct Chem 24:165–170
9. Beheshtian J, Peyghan AA, Bagheri Z (2012) Carbon nanotube functionalization with carboxylic derivatives: a DFT study. J Mol Model 19:391–396
10. Soltani A, Ahmadi Peyghan A, Bagheri Z (2013) H_2O_2 adsorption on the BN and SiC nanotubes: a DFT study. Phys E 48:176–180
11. Ahmadi A, Beheshtian J, Hadipour NL (2011) Chemisorption of NH_3 at the open ends of boron nitride nanotubes: a DFT study. Struct Chem 22(1):183–188

12. Pham HT, Duong LV, Tam NM, Pham-Ho MP, Nguyen MT (2014) The boron conundrum: bonding in the bowl B_{30} and B_{36}, fullerene B_{40} and triple ring B_{42} clusters. Chem Phys Lett 608:295–302
13. Li W-L, Chen Q, Tian W-J, Bai H, Zhao Y-F, Hu H-S, Li J, Zhai H-J, Li S-D, Wang L-S (2014) The B_{35} Cluster with a double-hexagonal vacancy: a new and more flexible structural motif for borophene. J Am Chem Soc 136(35):12257–12260
14. Li W-L, Pal R, Piazza ZA, Zeng XC, Wang L-S (2015) B27−: Appearance of the smallest planar boron cluster containing a hexagonal vacancy. J Chem Phys 142(20):204305
15. Piazza ZA, Hu H-S, Li W-L, Zhao Y-F, Li J, Wang L-S (2014) Planar hexagonal B_{36} as a potential basis for extended single-atom layer boron sheets. Nat Commun 5:3113–3117
16. Chen Q, Wei G-F, Tian W-J, Bai H, Liu Z-P, Zhai H-J, Li S-D (2014) Quasi-planar aromatic B 36 and B 36− clusters: all-boron analogues of coronene. Phys Chem Chem Phys 16(34):18282–18287
17. Liu C-S, Wang X, Ye X-J, Yan X, Zeng Z (2014) Curvature and ionization-induced reversible hydrogen storage in metalized hexagonal B_{36}. J Chem Phys 141(19):194306
18. Valadbeigi Y, Farrokhpour H, Tabrizchi M (2015) Adsorption of small gas molecules on B36 nanocluster. J Chem Sci 127(11): 2029–2038
19. Grimme S (2006) Semiempirical GGA-type density functional constructed with a long-range dispersion correction. J Comput Chem 27:1787–1799
20. Schmidt MW, Baldridge KK, Boatz JA, Elbert ST, Gordon MS, Jensen JH, Koseki S, Matsunaga N, Nguyen KA, Su S (1993) General atomic and molecular electronic structure system. J Comput Chem 14(11):1347–1363
21. Politzer P, Murray JS (2002) The fundamental nature and role of the electrostatic potential in atoms and molecules. Theor Chem Accounts 108(3):134–142
22. Politzer P, Murray JS (1991) Molecular electrostatic potentials and chemical reactivity. Rev Comput Chem 2:273–312
23. Wiberg KB (1997) Properties of some condensed aromatic systems. J Org Chem 62(17):5720–5727
24. Beheshtian J, Peyghan AA, Bagheri Z (2012) Detection of phosgene by Sc-doped BN nanotubes: a DFT study. Sensors Actuators B: Chem 171–172:846–852
25. Ahmadi A, Hadipour NL, Kamfiroozi M, Bagheri Z (2012) Theoretical study of aluminum nitride nanotubes for chemical sensing of formaldehyde. Sensors Actuators B: Chem 161:1025–1029
26. Peyghan AA, Hadipour NL, Bagheri Z (2013) Effects of Al doping and double-antisite defect on the adsorption of HCN on a BC2N nanotube: density functional theory studiess. J Phys Chem C 117(5):2427–2432
27. Baei MT, Peyghan AA, Bagheri Z (2012) A computational study of AlN nanotube as an oxygen detector. Chin Chem Lett 23:965–968
28. Baei MT, Peyghan AA, Bagheri Z, Tabar MB (2012) B-doping makes the carbon nanocones sensitive towards NO molecules. Phys Lett A 377:107–111
29. Beheshtian J, Peyghan AA, Bagheri Z, Kamfiroozi M (2012) Interaction of small molecules (NO, H2, N2, and CH4) with BN nanocluster surface. Struct Chem 23:1567–1572
30. Beheshtian J, Peyghan AA, Noei M (2013) Sensing behavior of Al and Si doped BC_3 graphenes to formaldehyde. Sensors Actuators B: Chem 181:829–834
31. Zhao Y, Truhlar DG (2006) A new local density functional for main-group thermochemistry, transition metal bonding, thermochemical kinetics, and noncovalent interactions. J Chem Phys 125(19):194101
32. Zhao Y, Truhlar DG (2008) The M06 suite of density functionals for main group thermochemistry, thermochemical kinetics, noncovalent interactions, excited states, and transition elements: two new functionals and systematic testing of four M06-class functionals and 12 other functionals. Theor Chem Accounts 120(1-3): 215–241
33. Zhao Y, Truhlar DG (2006) Density functional for spectroscopy: no long-range self-interaction error, good performance for Rydberg and charge-transfer states, and better performance on average than B3LYP for ground states. J Phys Chem A 110(49):13126–13130
34. Peyghan AA, Noei M (2014) The alkali and alkaline earth metal doped ZnO nanotubes: DFT studies. Phys B Condens Matter 432: 105–110
35. Beheshtian J, Peyghan AA, Bagheri Z, Tabar MB (2013) Density-functional calculations of HCN adsorption on the pristine and Si-doped graphynes. Struct Chem 25:1–7
36. Peyghan AA, Noei M (2014) Hydrogen fluoride on the pristine, Al and Si doped BC_2N nanotubes: a computational study. Comput Mater Sci 82:197–201
37. Beheshtian J, Peyghan AA, Bagheri Z (2013) Sensing behavior of Al-rich AlN nanotube toward hydrogen cyanide. J Mol Model 19(6):2197–2203
38. Cohen AJ, Mori-Sánchez P, Yang W (2008) Insights into current limitations of density functional theory. Science 321(5890):792–794
39. Peng C, Schlegel HB (1993) Combining synchronous transit and quasi-Newton methods to find transition states. Isr J Chem 33(4): 449–454